MULTIPACTOR DYNAMICS IN DIELECTRIC-LOADED ACCELERATOR STRUCTURES*

O. V. Sinitsyn, G. S. Nusinovich and T. M. Antonsen Jr.
IREAP, University of Maryland, College Park, MD 20742, U.S.A.

Abstract

In this paper the authors present results of three-dimensional analysis of multipactor in dielectric-loaded accelerator structures. The studies are aimed at checking some assumptions that were used in previous two-dimensional theory. In particular, it is demonstrated that the spatial distribution of charged particles can be azimuthally non-uniform which suggests using a more complex space charge model in some cases. Also, it is shown that the particle axial velocity components can be making a substantial contribution to particle energy and should not be ignored in future studies.

INTRODUCTION

Multipactor (MP) manifests itself as a rapid growth of the number of secondary electrons emitted from a solid surface in the presence of the RF field under vacuum conditions. The secondary electrons appear as the result of impacts of energetic primary electrons accelerated by the RF field. MP occurs in various microwave and RF systems and usually significantly degrades their performance. In particular, it generates RF noise, reduces RF power flow, changes device impedance, stimulates RF breakdown, etc. Therefore theoretical and experimental studies of MP are of great interest to researchers working in related areas of physics and engineering. In this paper, MP in the dielectric-loaded accelerator (DLA) structures is studied. The starting point for this work was theoretical and experimental studies of such structures jointly done by Argonne National Laboratory and Naval Research Laboratory [1-3]. In the theoretical model developed during those studies the space charge field created by secondary electrons was taken into account as a parameter. We have developed a non-stationary 2D model of MP in which the space-charge field was taken into account self-consistently [4]. We compared results predicted by that model with the experimental ones obtained during extensive studies of DLA structures performed by ANL, NRL, SLAC National Accelerator Laboratory and Euclid TechLabs, LLC [5]. Good agreement between both data was demonstrated for the tube with alumina liner and tubes with quartz liner of large diameter. However, for quartz tubes of smaller diameter a large discrepancy was observed [6]. There could be several reasons that would lead to such disagreement. First, in our 2D model we were assuming that the MP was occurring mainly due to the effect of the radial component of the RF electric field. Therefore, in our simulations we were neglecting the axial motion of electrons that in some cases could be making a substantial contribution to the total energy of the particles. Secondly, we were assuming that space charge distribution of secondary electrons was azimuthally uniform which was allowing us to use a simple model for the calculation of the space charge fields. In this paper we are using a simple 3D model to verify whether those assumptions were valid. The paper is organized as follows: in the next section we provide a brief description of the model used in our studies, in the 'Results' section we show some results of our simulations and in the last section we give a summary.

*This work is supported by the Office of High Energy Physics of the US Department of Energy.

FORMALISM

The motion of an electron in the presence of the field of the TM_{01} forward wave can be described by the following set of equations [7]:

$$\frac{d\tilde{v}_r}{d\tilde{t}} = \frac{\tilde{v}_{\phi 0}^2}{\tilde{r}^3} - \frac{\alpha}{\rho_1}(\tilde{v}_z\tilde{\omega}^2 - \rho_z) I_1(\rho_1\tilde{r})\sin(\tilde{t} - \rho_z\tilde{z}) \quad (1)$$

$$\tilde{v}_\phi = \frac{\tilde{v}_{\phi 0}}{\tilde{r}} \quad (2)$$

$$\frac{d\tilde{v}_z}{d\tilde{t}} = -\alpha\left(I_0(\rho_1\tilde{r})\cos(\tilde{t} - \rho_z\tilde{z}) - \frac{\tilde{v}_r\tilde{\omega}^2}{\rho_1} I_1(\rho_1\tilde{r})\sin(\tilde{t} - \rho_z\tilde{z})\right). \quad (3)$$

These equations do not take into account space charge forces and, therefore, can be used only for describing the initial stage of MP when the space charge effects are small. In Eqs 1-3, $\tilde{r} = r/a$ is the normalized radial coordinate of the particle (a is the inner radius of the dielectric liner), ϕ and $\tilde{z} = z/a$ are its angular and normalized axial coordinates, respectively. $\tilde{v}_r = v_r/a\omega$, $\tilde{v}_\phi = v_\phi/a\omega$ and $\tilde{v}_z = v_z/a\omega$ are the radial, angular and axial normalized electron velocities, respectively (here $\omega = 2\pi f$ is the wave frequency), $\alpha = eE_{rf}/m\omega^2 a$ is the normalized amplitude of the RF signal, where e and m are the electron charge and mass, respectively. Also, in these equations, $\rho_1 = |k_{\perp 1}|a$, $\rho_z = k_z a$, $\tilde{\omega} = \omega a/c$ are the normalized transverse wavenumber in the vacuum region, normalized axial wavenumber and normalized frequency of the wave. The seed particles appear on the dielectric surface with a certain periodicity which we took equal to 0.25π in our calculations. We assume that they have random initial energies E_0 and emission angles θ_e (in

both $r-\phi$ and $z-r$ planes) obeying the following distribution functions:

$$f(E_0) = \frac{E_0}{E_{0m}^2}\exp(-E_0/E_{0m}) \quad (4)$$

$$g(\theta_e) = \frac{1}{2}\sin(\theta_e), \quad 0 < \theta_e < \pi, \quad (5)$$

where E_{0m} is the energy corresponding to the peak of the energy distribution function. After leaving the surface the particle continues its motion in the vacuum region till it impacts the wall. Based on its impact energy and impact angle, the secondary emission yield is calculated. In our simulations we employ the well-known Vaughan SEY model [8] which uses four parameters to characterize a given material: $\delta_{\max 0}$ - maximum secondary yield at normal incidence, $E_{\max 0}$ - impact energy corresponding to $\delta_{\max 0}$, $k_{s\delta}$ - material smoothness factor for δ and k_{sE} - material smoothness factor for E.

RESULTS

First, we performed simulations for the alumina tube which has the following parameters: a = 5 mm, b = 7.185 mm, ε_d = 9.4 [1]. The accelerating gradient on the axis $E_{rf} = 5$ MV/m, the parameters of the secondary yield model are $\delta_{\max 0} = 5$ and $E_{\max 0} = 600$ eV in these calculations [9]. Fig. 1 shows the distribution of macroparticles in the plane of angular and axial

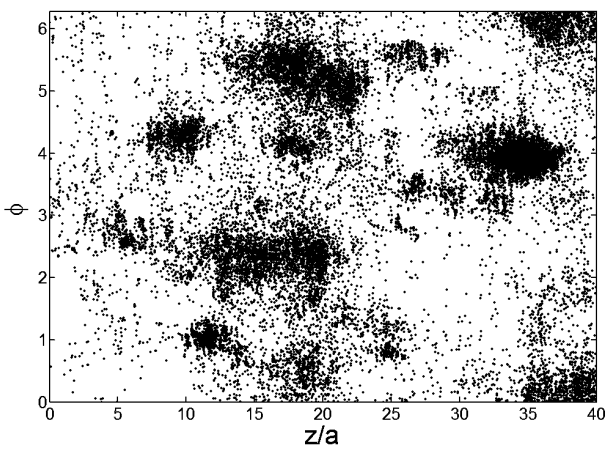

Figure 1: Locations of macroparticles on the plane of their angular and axial coordinates for the alumina tube.

coordinates obtained at t = 5.46 ns after the beginning of calculations. One may notice that the particles are distributed non-uniformly on the plane and that there are regions where their density is significantly higher.

Such calculations were also done for the tubes with quartz liner. Fig. 2 shows similar distribution for the tube with the following specifications: a = 8.97 mm, b = 12.08 mm, ε_d = 3.75 [5]. The instant of time at which

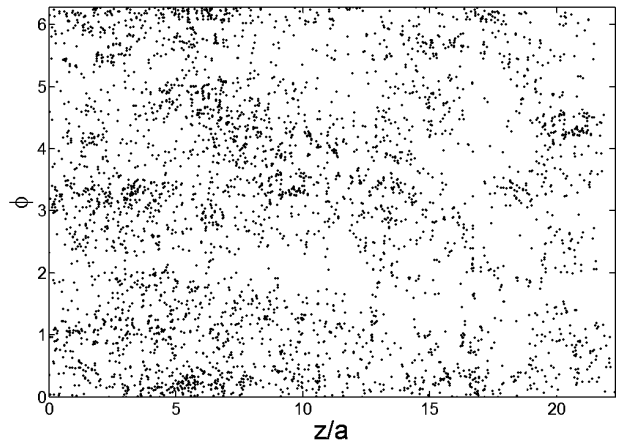

Figure 2: Locations of macroparticles on the plane of their angular and axial coordinate for the quartz tube with inner radius a = 8.97 mm and outer radius b = 12.08 mm.

the data was obtained was t = 15.27 ns. The accelerating gradient is $E_{rf} = 5$ MV/m and the secondary yield model parameters are $\delta_{\max 0} = 2.6$ and $E_{\max 0} = 400$ eV in this case [9]. One may see that the particles are distributed much more uniformly on the plane in this case. The non-uniform distribution in the case of alumina tube could be attributed to the fact that alumina has a higher secondary emission yield value in comparison with quartz. Therefore, one primary electron impacting alumina surface can generate many secondaries, which multiply quickly under the influence of the RF field around the location of the impact. If the seed particles appear with relatively low rate, one may see such spots of higher density in the spatial particle distribution.

To understand whether axial velocities of the particles are important (as mentioned, we ignored those in our 2D model), we analyzed distributions of particle velocity components. Some results of such studies are shown in Fig. 3, which demonstrates histograms for absolute values of two normalized velocity components in the alumina tube. Figures 3a and 3b correspond to the histograms for $|\tilde{v}_r|$ and $|\tilde{v}_z|$, respectively. The histograms were obtained at t = 5.46 ns. We didn't include the histogram for $|\tilde{v}_\phi|$ since this velocity component is relatively small in comparison with radial and axial ones. One may see that the particles have a significant axial velocity component, which can be even larger than the radial one. We performed similar calculations for the quartz tube with the following parameters: a = 3 mm, b = 7.372 mm, ε_d = 3.75 [5]. The corresponding results are shown in Fig. 4. As one may see, the axial velocity component of a particle in this case can be much larger than the radial one. In particular, the maximum value of the radial component can be about 0.05, whereas the axial velocity can reach values of about 0.12. Also the number of the particles with large axial velocities is substantial. This shows that the axial velocity component makes a great

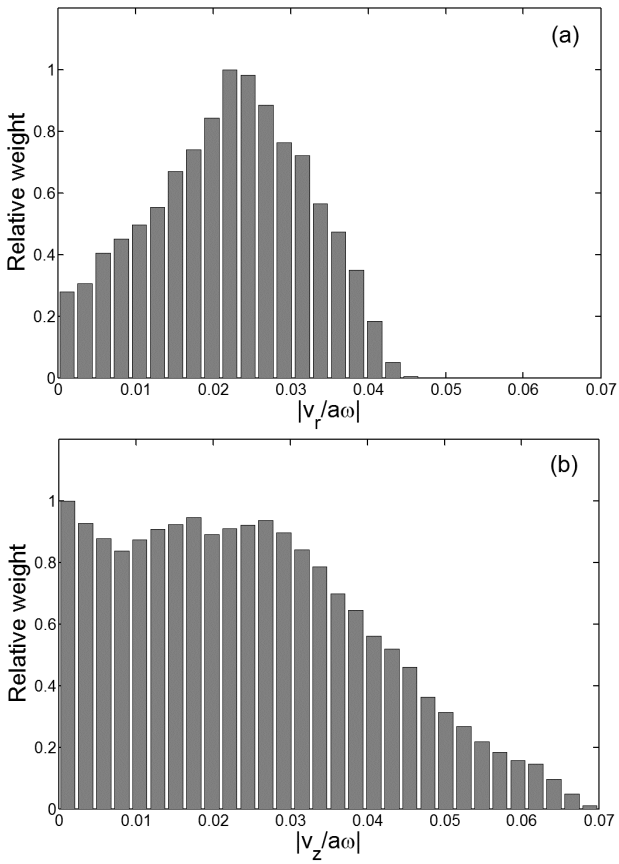

Figure 3: Histograms for absolute values of radial and axial velocity components obtained for the alumina-based structure.

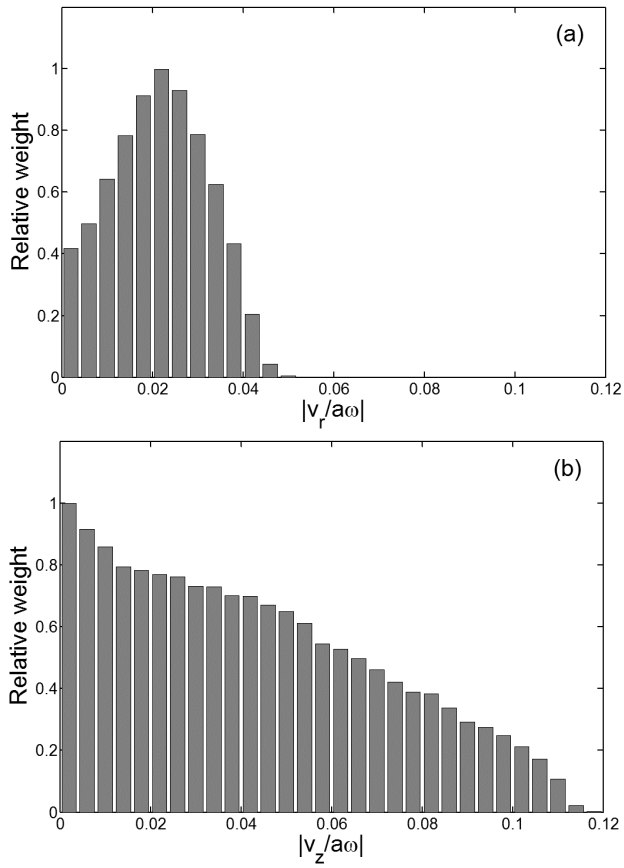

Figure 4: Histograms for absolute values of radial and axial velocity components obtained for the quartz structure with inner radius a = 3 mm and outer radius b = 7.372 mm.

contribution to the total energy of the particle and should not be ignored in the analysis.

SUMMARY

We have developed a simple 3D model of MP that allowed us to check the assumptions that were used in our 2D studies. In particular, we have demonstrated that the spatial distribution of charged particles can be azimuthally non-uniform and that the simple space charge model used in our 2D studies [4] should be used with caution. A more advanced model might be more suitable in some situations.

We have also demonstrated that particles might have a large axial velocity component that contributes significantly to their total kinetic energy. Since the secondary emission yield depends on the particle impact energy, its accurate evaluation is very important. Therefore, the axial motion of the particle should be included in future theoretical studies of MP in DLA structures.

REFERENCES

[1] J. G. Power, W. Gai, S. H. Gold et al., *Phys. Rev. Lett.*, **92**, 164801 (2004).
[2] J. G. Power and S. H. Gold, *AIP Conf. Proc.*, **877**, 362 (2006).
[3] C. Jing, W. Gai, J. G. Power et al., *IEEE Trans. Plasma Sci.*, **33**, No. 4, 2005, pp. 1155-1160.
[4] O. V. Sinitsyn, G. S. Nusinovich and T. M. Antonsen, Jr., *Phys. Plasmas*, **16**, 073102 (2009).
[5] C. Jing, W. Gai, J. G. Power et al., *IEEE Trans. Plasma Sci.*, **38**, No. 6, 2010, pp. 1354-1360.
[6] O. V. Sinitsyn, G. S. Nusinovich and T. M. Antonsen, Jr., AIP Conf. Proc., **1299**, 302 (2010).
[7] O. V. Sinitsyn, G. S. Nusinovich and T. M. Antonsen, Jr., "2D and 3D multipactor modeling in dielectric-loaded accelerator structures," 52nd Annual Meeting of the APS Division of Plasma Physics, Nov. 8-12, 2010, Chicago, IL.
[8] J. R. M. Vaughan, IEEE Trans. Electron Devices, 36, 1963 (1989).
[9] O. Hachenberg and W. Brauer, *Advances in Electronics and Electron Physics*, edited by L. Marton, Academic Press, New York, 1959, pp. 413-499.